



Hydrological control of large hurricane-induced lahars: evidence from rainfall-runoff modeling, seismic and video monitoring

Lucia Capra¹, Velio Coviello^{1,2}, Lorenzo Borselli³, Víctor-Hugo Márquez-Ramírez¹, and Raul Arámbula-Mendoza⁴

¹Centro de Geociencias, Universidad Nacional Autónoma de México (UNAM), Campus Juriquilla, Querétaro, Mexico

²Free University of Bozen-Bolzano, Facoltà di Scienze e Tecnologie, Bolzano, Italy

³Instituto de Geología, Universidad Autónoma de San Luis Potosí, San Luis Potosí, Mexico

⁴Centro Universitario de Estudios e Investigaciones en Vulcanología (CUEIV), Universidad de Colima, Colima, Mexico

Correspondence: Lucia Capra (lcapra@geociencias.unam.mx)

Received: 8 October 2017 – Discussion started: 13 October 2017

Revised: 29 January 2018 – Accepted: 30 January 2018 – Published: 9 March 2018

Abstract. The Volcán de Colima, one of the most active volcanoes in Mexico, is commonly affected by tropical rains related to hurricanes that form over the Pacific Ocean. In 2011, 2013 and 2015 hurricanes Jova, Manuel and Patricia, respectively, triggered tropical storms that deposited up to 400 mm of rain in 36 h, with maximum intensities of 50 mm h^{-1} . The effects were devastating, with the formation of multiple lahars along La Lumbre and Montegrande ravines, which are the most active channels in sediment delivery on the south-southwest flank of the volcano. Deep erosion along the river channels and several marginal landslides were observed, and the arrival of block-rich flow fronts resulted in damages to bridges and paved roads in the distal reaches of the ravines. The temporal sequence of these flow events is reconstructed and analyzed using monitoring data (including video images, seismic records and rainfall data) with respect to the rainfall characteristics and the hydrologic response of the watersheds based on rainfall-runoff numerical simulation. For the studied events, lahars occurred 5–6 h after the onset of rainfall, lasted several hours and were characterized by several pulses with block-rich fronts and a maximum flow discharge of $900 \text{ m}^3 \text{ s}^{-1}$. Rainfall-runoff simulations were performed using the SCS-curve number and the Green–Ampt infiltration models, providing a similar result in the detection of simulated maximum watershed peaks discharge. Results show different behavior for the arrival times of the first lahar pulses that correlate with the simulated catchment's peak discharge for La Lumbre ravine and with the peaks in rainfall intensity for Montegrande ravine. This different behavior is

related to the area and shape of the two watersheds. Nevertheless, in all analyzed cases, the largest lahar pulse always corresponds with the last one and correlates with the simulated maximum peak discharge of these catchments. Data presented here show that flow pulses within a lahar are not randomly distributed in time, and they can be correlated with rainfall peak intensity and/or watershed discharge, depending on the watershed area and shape. This outcome has important implications for hazard assessment during extreme hydro-meteorological events, as it could help in providing real-time alerts. A theoretical rainfall distribution curve was designed for Volcán de Colima based on the rainfall and time distribution of hurricanes Manuel and Patricia. This can be used to run simulations using weather forecasts prior to the actual event, in order to estimate the arrival time of main lahar pulses, usually characterized by block-rich fronts, which are responsible for most of the damage to infrastructure and loss of goods and lives.

1 Introduction

In recent years hurricanes have had catastrophic effects on volcanoes in the tropics through the triggering of lahars (sediment–water gravity-driven flows on volcanoes). One of the most recent episodes is represented by Hurricane Ida in El Salvador in 2009, that caused several landslides and debris flows from the Chichontepec Volcano, killing 124 people. In

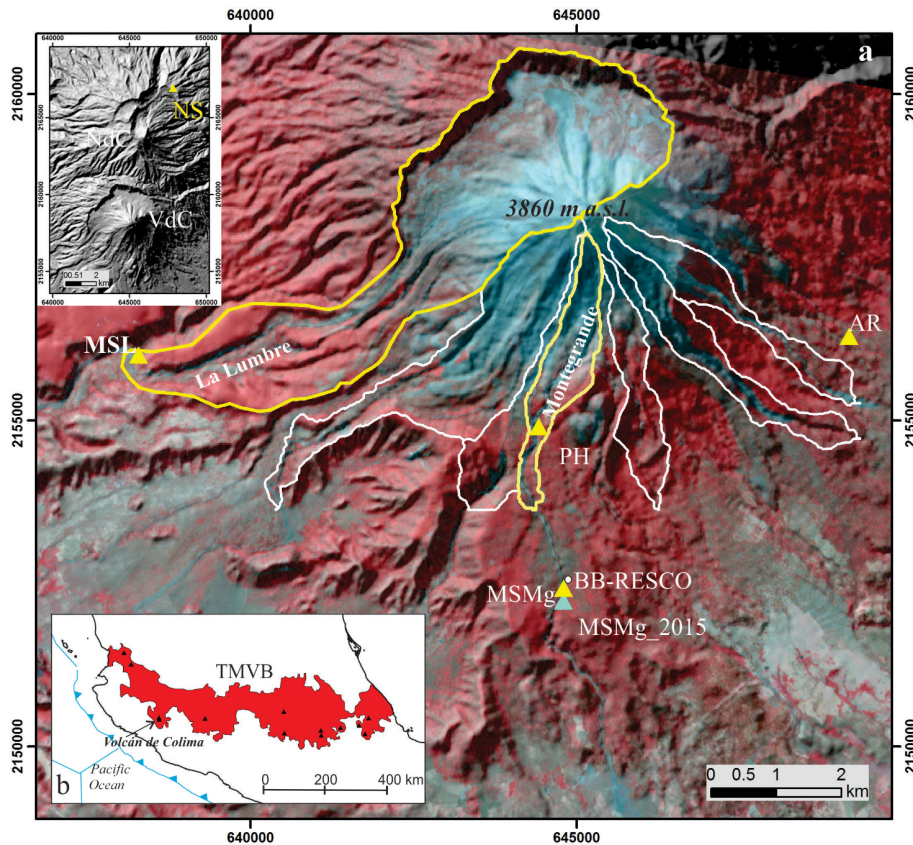


Figure 1. (a) Aster image (4, 5 and 7 bands in RGB combination) wherein the main watersheds at Volcán de Colima are represented. The locations of the monitoring stations are indicated. The inset shows the location of the rain gauge of the Meteorological National Service at the summit of the Nevado de Colima Volcano. (b) Sketch map of the Trans-Mexican Volcanic Belt (TMVB) and the Volcán de Colima location. Black triangles denote the main active volcanoes in Mexico.

1998, Hurricane Mitch triggered the collapse of a small portion of the inactive Casita Volcano (Nicaragua), initiating a landslide that suddenly transformed into a lahar, devastating several towns and killing 2000 people (Van Wyk Vries et al., 2000; Scott et al., 2005). A similar event was observed in 2005, when tropical storm Stan triggered landslides and debris flows from the Tolimán Volcano (Guatemala), causing more than 400 fatalities in the Panabaj community (Sheridan et al., 2007). Other examples can be found at the Pinatubo (Philippines), Merapi and Semeru (Indonesia), Soufrière Hills (Montserrat) and Tungurahua (Ecuador) volcanoes, where tropical storms and heavy rainfall seasons have triggered high-frequency lahar events (Umbal and Rodolfo, 1996; Lavigne et al., 2000; Lavigne and Thouret, 2002; Barclay et al., 2007; Dumaisnil et al., 2010; Doyle et al., 2010; de Bélizal et al., 2013; Jones et al., 2015).

Volcán de Colima ($19^{\circ}31'N$, $103^{\circ}37'W$; 3860 m a.s.l.; Fig. 1), one of the most active volcanoes in Mexico, is periodically exposed to intense seasonal rainfalls that are responsible for the occurrence of lahars from June to late October (Davila et al., 2007; Capra et al., 2010; Vázquez et al., 2016a). Lahars usually affect areas as far as 15 km from the

summit of the volcano, resulting in damage to bridges and electrical power towers (Capra et al., 2010). Lahars are more frequent just after eruptive episodes, such as dome collapses that create block and ash flow deposits (Davila et al., 2007; Vázquez et al., 2016b). Several hurricanes commonly hit the Pacific Coast each year and proceed inland as tropical rainstorms, thus reaching the Volcán de Colima area. In particular, in 2011, 2013 and 2015 Hurricanes Jova, Manuel and Patricia, respectively, triggered long-lasting lahars along main ravines draining the edifice, causing severe damage to roads and bridges, and leaving communities in a radius of 15 km from the volcano cut off for several days.

Previous work (Davila et al., 2007; Capra et al., 2010) analyzed lahar frequency at Volcán de Colima in relation to eruptive activity and rainfall characteristics. Lahars are more frequent at the beginning of the rainy season, during short (< 1 h) non-stationary rainfall events, with variable rainfall intensities and only 10 mm of accumulated rainfall. This behavior has been attributed to a hydrophobic effect of soils on the volcano slope (Capra et al., 2010). In contrast, in the late rainy season, when tropical rainstorms are common, lahars are triggered depending on the 3 day antecedent rainfall and

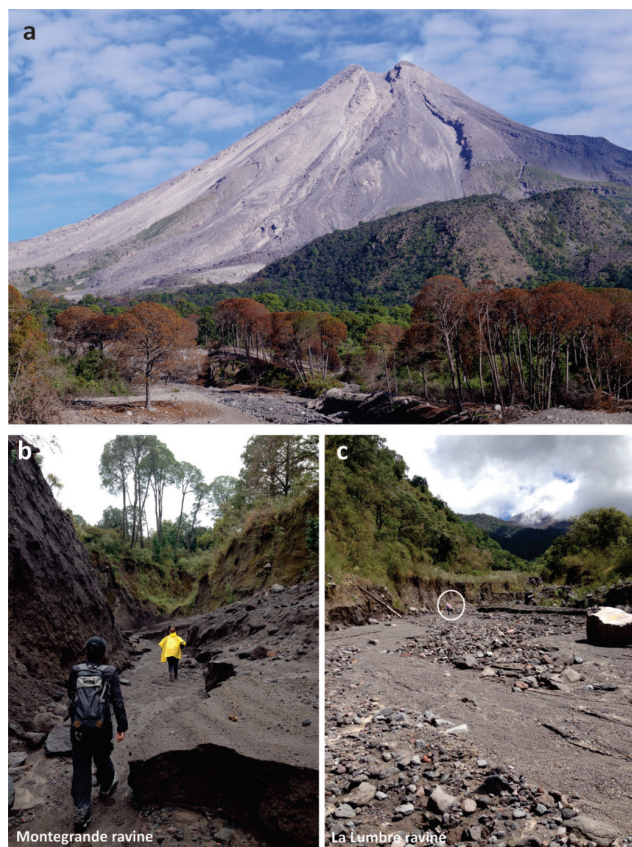


Figure 2. (a) Panoramic view of the Volcán de Colima showing the unvegetated main cone mostly composed of loose volcanic fragments. (b) Montegrande and (c) La Lumbre ravines in the middle reach, where it is possible to observe the main channel flanked by 10–15 m high terraces mainly constituted by debris avalanche deposits.

with intensities that increase as the total rainfall amount increases (Capra et al., 2010). The lahar catalog used for these previous studies was based only on seismic data. Since 2011 a visual monitoring system has been installed on the Montegrande and La Lumbre ravines (Fig. 1), based on which a quantitative characterization of some events (i.e. type of flow, velocity, flow discharge, flow fluctuation) has been possible (i.e., Vázquez et al., 2016a; Coviello et al., 2018). The aim of the present paper is to better understand the initiation processes of large lahars and their dynamic behavior, especially during hurricane events, when more damage has been observed in inhabited areas. In particular, the arrival time of the main lahar's front or surge at the monitoring stations is analyzed with respect to rainfall characteristics (rain accumulation and intensity) and in relation to the watershed's hydrological response based on a rainfall-runoff numerical simulation.

The occurrence of discrete surges within debris flows and lahars has been attributed to spatially and temporally distributed sediment sources, temporary damming, progressive

entrainment of bed material or change in slope angle (Iverson 1997; Marchi et al. 2002; Takahashi 2007; Zanuttigh and Lamberti 2007; Doyle et al., 2010; Kean et al., 2013). Without excluding previous models, data from large lahars triggered by Hurricanes Jova, Manuel and Patricia show that the main pulses within a lahar are not randomly distributed in time, and that they can be correlated with rainfall peak intensity and/or watershed discharge, depending on (1) watershed shape, and (2) hydrophobic behavior, subject to the antecedent soil moisture. These lahars are also compared with a flow triggered by an extraordinary hydro-meteorological event that occurred at the beginning of the rain season (11 June 2013), to better show the drastic change on lahar initiation due to the hydrophobic effect of soils at Volcán de Colima. Based on rainfall distribution over time for the analyzed events, a theoretical rainfall distribution curve is designed here, which can be used to run simulations prior to an event in order to have an estimation of the arrival of the main pulses when the weather forecast is available. Results presented here have important implications for hazard assessment during extreme hydro-meteorological events and can be used as a complementary tool to develop an early warning system (EWS) for lahars on tropical volcanoes.

2 Methods and data

2.1 La Lumbre and Montegrande watersheds

The source area of rain-triggered lahars at Volcán de Colima corresponds to the uppermost unvegetated portion of the cone (Figs. 1 and 2a), with slopes between 35 and 20° that also correspond with an area of high connectivity, being prone to rill formation and erosive processes (Ortiz-Rodriguez et al., 2017). The channels along main ravines have slopes that vary from 15° proximally, up to a maximum of 4° in the more distal reaches. They are flanked by densely vegetated terraces, up to 15 m high average, that consist of debris avalanche and pyroclastic deposits from past eruptions (Fig. 2b and c) (Cortes et al., 2010; Roverato et al., 2011). Seven major watersheds feed the main ravines draining from the volcano on the southern side (Fig. 1). La Lumbre is the largest watershed, with a total area of 14 km², and Montegrande is representative of the other catchments with an area of 2 km² (Fig. 1). Aside from the difference in total area, the Montegrande and La Lumbre watersheds are quite different in geometry. Montegrande catchment is elongated, with a maximum width of 800 m (300 m average). In contrast, the proximal portion of La Lumbre catchment includes the entire north-west slope of the cone, before elongating towards the south-west, up to 1500 m in width. These differences in area and shape can be correlated with a different water discharge response during a rainfall event. In circular drainages, i.e., the proximal portion of La Lumbre watershed, all points are equidistant from the main channel so that all of the precipi-

Table 1. Data collected for the events studied in this paper.

Event	Ravine	Seismic record	Image record	Rain gauge	Total rain (mm)	Max. rain intensity (mm h^{-1})
Jova, 12 October 2011	Monte grande	×		MSMg	240	43
Manuel 15 September 2013	Monte grande	×		MSMg	300	32
Patricia 23 October 2015	Lumbre	×	×	NS	400	37
11 June 2013	Monte grande	×	×	MSMg	120	140

tation reaches the river at the same time, concentrating as a large volume of water. In contrast, in a more elongated basin, lateral drainages quickly drain water into the main channel at different points resulting in a lower total discharge. The Gravelius's index K_G (Gravelius, 1914; Bendjoudi and Hubert 2002), which is defined as the relation between the perimeter of the watershed (P) and that of a circle having a surface equal to that of a watershed (A) as follows:

$$K_G = \frac{P}{2\sqrt{\pi A}}, \quad (1)$$

here is estimated for Monte grande watershed and for the upper, circular portion of La Lumbre watershed, obtaining values of 1.7 and 1.1, respectively. The lower the value, the more regular the basin's perimeter and the more prone it is to present high runoff peaks. Based on these considerations, at La Lumbre watershed a larger volume of water concentrates along the main channel, because of its larger surface and circular shape, but after a larger period of time relative to the Monte grande ravine, where a minor volume of water quickly reaches the main drainage area.

2.2 Lahar monitoring at Volcán de Colima

In 2007, a monitoring program was implemented at Volcán de Colima. Initially, two rain gauges were installed to study lahar initiation (AR and PH sites, Fig. 1) and lahar propagation was detected using the broadband seismic stations of RESCO, the seismological network of Colima University (Davila et al., 2007; Zobin et al., 2009; Capra et al., 2010). Two monitoring stations specifically designed for studying lahar activity were installed later, in 2011 at the Monte grande ravine and in 2013 at La Lumbre ravine (MSMg and MSL respectively, Fig. 1). Both stations consist of a 12 m high tower with a directional antenna transmitting data in real time to RESCO facilities, a camcorder recording images every 2–4 s with a 704×480 pixel resolution, a rain gauge coupled with a soil moisture sensor and a 10 Hz geophone (Vázquez et al., 2016a; Coviello et al., 2018). The rain gauge (HOBO RG3)

records rain accumulation at 1 min intervals. At Monte grande ravine seismic data are also obtained from a three component Guralp CMG-6TD broadband seismometer installed 500 m upstream from the monitoring site, sampling at 100 Hz (BB-RESCO, Fig. 1).

The Monte grande station detected lahars during the 2011 Jova and 2013 Manuel events, while lahars triggered during Hurricane Patricia in 2015 were only recorded by La Lumbre station (Table 1). In 2011, only the MSMg site was operational (as the BB-RESCO station), and recorded the seismic signal of lahars associated with the Jova and Manuel events. No images are available as both events occurred during the night. The MSL station began to operate at the end of 2013 and was able to record lahars associated with Hurricane Patricia along the La Lumbre ravine (images and geophone data). In contrast, in 2015 the MSMg site was destroyed by pyroclastic flows during the explosive activity of 10–11 July, and in October 2015 the new station (MSMg_2015) was still under construction. Only a few pictures were acquired and they are of low quality because of the abundant steam generated by hot lahars, as they originated from the remobilization of fresh pyroclastic flow deposits (Capra et al., 2016). The 11 June 2013 event was perfectly captured by the camera installed at the MSMg site and the BB-RESCO recorded its seismic signal.

The seismic signal is analyzed here to detect the arrival of main flow fronts and to estimate the discharge variation. For this only the amplitude of the signal is considered, which can be correlated with the variation in the maximum peak flow discharge (Doyle et al., 2010; Vázquez et al., 2016a). In particular, for lahars at Volcán de Colima a correlation between the maximum peaks in amplitude and the maximum peak in flow discharge was found (Fig. 5 in Vázquez et al., 2016a). Fluctuation in seismic energy along the vertical component reflects variation in flow discharge.

The seismic record is compared here with the available images to identify the main changes in lahar dynamics. All the lahars analyzed here correspond to multi-pulse events as classified by Vázquez et al. (2016a). They consist of long

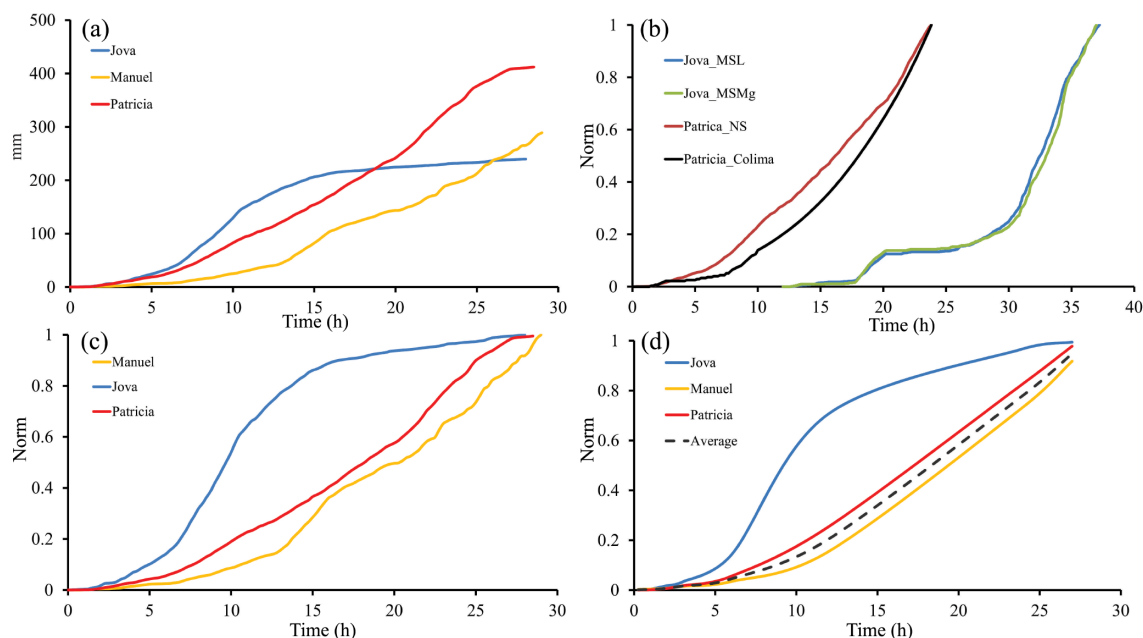


Figure 3. (a) Cumulative values of rainfall of hurricanes Jova, Manuel and Patricia calculated at 10 min intervals. (b) Normalized rainfall curves for the Jova and Patricia events as gathered from two different stations, pointing to a quasi-stationary rainfall behavior. (c) Normalized values of cumulative rainfall curves. (d) Normalized curve of total rainfalls cumulated at 15, 30, 60 min and 1, 3, 6, 12, 18, 24, 27 h. Dotted line represents the average value between hurricanes Manuel and Patricia.

lasting lahars presenting several pulses, each characterized by a block-rich front followed by the main body and diluted tail showing continuous changes in flow discharge. A detailed seismic description of lahar types at Volcán de Colima is available in Vázquez et al. (2016a). Here we focus on the number of main flow peaks and their arrival times.

2.3 The hydro-meteorological events

Hurricane Jova formed over the Pacific Ocean, hit the Pacific coast on 12 October 2011 as a category 2 event, and traveled inland toward Volcán de Colima. The hurricane arrived as a tropical storm at the town of Coquimatlán, 10 km SW of the city of Colima with winds of up to 140 km h^{-1} , and 240 mm of rain falling over 24 h (Fig. 3a). Severe damage was registered in inhabited areas, including the city of Colima, where floods damaged roads, bridges and buildings.

Hurricane Manuel (category 1), hit the Pacific coast on 15 September 2013 causing severe damage to the mountainous region of Guerrero, triggering several landslides that caused up to 96 deaths and left several villages cut off, while thousands of tourists were trapped at Acapulco and Ixtapa international airports. At Volcán de Colima rain started on 15 September with more than 300 mm falling over more than 30 h (Fig. 3a).

Hurricane Patricia in 2015 was considered the strongest hurricane on record to effect Mexico. The system began to develop on 18 October over the Pacific Ocean, strengthened

into a hurricane shortly after 00:00 GMT on 22 October, and early on 23 October it reached its maximum category of 5, before losing strength as it moved onto the Sierra Madre Occidental range. Landfall occurred around 23:00 GMT on 22 October along the coast of the Mexican state of Jalisco near Playa Cuixmala, about 60 km west-northwest of Manzanillo. On the morning of the 23 October 2015 it continued to rapidly weaken. In Colima town, up to 400 mm of rain fell over the 30 h after the morning of 23 October (Fig. 3a). Lahars along the Montegrando ravine were hot as they originated from the erosion of pyroclastic flow deposits that originated from the 10–11 July 2015 eruption. Severe damage affected Colima town and areas surrounding the volcano. A bridge along the interstate was destroyed, cutting of La Berrera village and interrupting traffic between Colima and Jalisco state.

Rainfall during hurricanes

Rainfall data were obtained from different rain gauge stations (Table 1 and Fig. 1). In particular, for the events studied at Montegrando ravine, rainfall data came from the rain gauge installed at MSMg, while for the Patricia event the more proximal available rain station is located at the top of the Nevado de Colima volcano (NS, Fig. 1). It is worth mentioning that at Volcán de Colima, during stationary rainfall events associated with hurricanes, no important differences in rainfall duration and intensity are detected at re-

Table 2. Normalized accumulated rains at progressive time steps.

Event/time (h)	0.25	0.5	1	2	3	6	12	24	27
Jova	0.0011	0.0016	0.0035	0.0172	0.0329	0.1411	0.7073	0.968	0.9943
Manuel	0.0023	0.0035	0.0042	0.0072	0.0151	0.0341	0.1548	0.735	0.9181
Patricia	0.0002	0.0004	0.0009	0.0062	0.0174	0.0556	0.2544	0.829	0.9782
Average	0.00125	0.00195	0.00255	0.0067	0.01625	0.04485	0.2046	0.782	0.9481

The average values refer to hurricanes Manuel and Patricia.

gional scale. For instance, the measured rainfall associated with Hurricane Jova was alike at two rain gauges located more than 7 km apart (MSMg and MSL), and during Hurricane Patricia the same duration and intensity values were recorded by station NS and a station located in the Colima town, 30 km S from the volcano summit (Fig. 3b).

Rainfall during hurricanes Patricia and Manuel shows similar behavior, with progressive rain accumulation over 28–30 h; in contrast, during Hurricane Jova, 200 mm of rain fell in less than 15 h, with only another 40 mm falling during the following 13 h (Fig. 3a). These differences are more evident plotting the 10 min accumulated value normalized over the total accumulated rainfall (Fig. 3c). Average rainfall intensities calculated over a 10 min interval range from 32 to 37 mm h⁻¹ for Manuel and Patricia events respectively and up to 43 mm h⁻¹ for the Hurricane Jova (Table 1). Finally rainfall values were calculated at selected time intervals (0.25, 0.5, 0.75, 1, 3, 6, 12, 18, 24, 27 h) to design possible storm rainfall distributions, based on tropical rains associated with hurricanes recorded historically at Volcán de Colima (Table 2). Considering the similar behavior of the Manuel and Patricia rainfalls, a theoretical rainfall distribution curve can be designed considering their average values (Fig. 3d) (i.e., NRCS, 2008), based on which a forecast analysis can be performed, as will be discussed below.

2.4 Rainfall-runoff modeling

To better understand the lahar behavior and duration during extreme hydro-meteorological events at Volcán de Colima, rainfall-runoff simulations were performed with Flo-2D code (O'Brien et al., 1993). The Flo-2D code routes the overland flow as discretized shallow sheet flow using the Green–Ampt or the SCS curve number (or combined) infiltration models. For the present work, the SCS curve number (SCS-CN, i.e., Mishra and Singh, 2003) was selected for the analysis and a comparison between both infiltration models is presented below. The rainfall is applied to the entire watershed, without spatial variability because we are dealing with large-scale, long duration hurricane-induced rainfall. This rainfall is discretized as a cumulative percent of the total precipitation each 10 min. With the SCS-CN model, the volume of water runoff produced for the simulated precipitation is estimated through a single parameter, i.e., the curve number

(CN). This parameter summarizes the influence of both the superficial aspects and deep soil features, including the saturated hydraulic conductivity, type of land use, and humidity before the precipitation event (for an accurate description of the origin of the method see Rallison, 1980; Ponce and Hawkins, 1996). A similar approach was previously used for modeling debris flow initiation mechanisms (i.e., Gentile et al., 2006; Llanes et al., 2015). To apply the SCS-CN model, it is necessary to classify the soil in to one of four groups, each identifying a different potential runoff generation (A, B, C, D; USDA-NRCS, 2007). The watershed of La Lumbre and Montegrande ravines were subdivided into two main zones: (1) the unvegetated upper cone and the main channel that consists of unconsolidated pyroclastic material with large boulders embedded in a sandy to silty matrix, and (2) the vegetated lateral terraces. Lateral terraces consist of old pyroclastic sequences with incipient soils and are vegetated with pine trees and sparse bushes. Based on these observations, soils were classified between group A and B (Bartolini and Borselli, 2009). CN values for the vegetated terraces and for the nude soils were estimated at 75 and 80, respectively (in the wet season, Hawkins et al., 1985; Ferrer-Julia et al., 2003). To perform a simulation with the FLO-2D code, two polygons were traced to delimit the un-vegetated portion of the cone from the vegetated area of the watershed, and at each polygon the relative CN value was assigned. At the apex of each watershed a barrier of outflow points were defined to obtain the values of the simulated watershed discharge computed at each 0.1 h. The simulation was performed with a 20 m digital elevation model. One of the limitations of the SCS method is that it does not consider the effect of the rainfall intensity on the infiltration. In addition, since no measurements of water discharge are available at both La Lumbre and Montegrande basins, it is difficult to calibrate the simulations here presented. To investigate the SCS-CN model uncertainties, the Green–Ampt (1911) model (G–A), sensitive to the rainfall intensity, was also applied and the results were compared with the outcome of the SCS-CN model. For the G–A method, the main input parameters are the saturated hydraulic conductivity (Ks), the soil suction and volumetric moisture deficiency. The Ks is a key factor in the estimation of infiltration rates and exerts a notable influence on runoff calculations, therefore requiring great care in its mea-

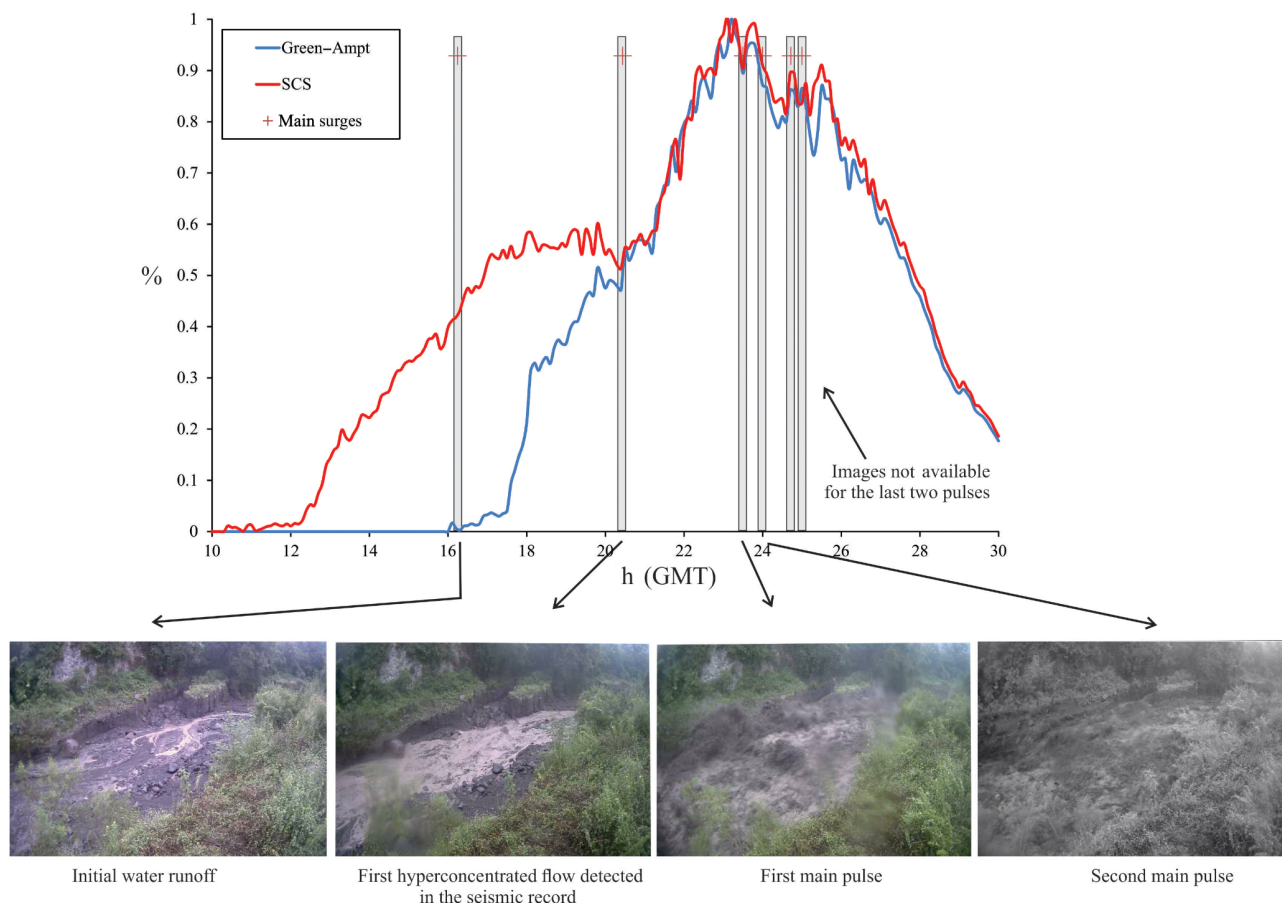


Figure 4. Comparison of simulated watershed discharge curves based on SCS-NC and G–A infiltration models. Qualitative calibration is here proposed based on the flow discharge as observed in the video images captured at the MSL site.

surement (Grimaldi et al., 2013). The input values can be extrapolated from tables or directly measured with field experiments. Based on the textural characteristics of soils and the type of vegetation at Volcán de Colima, input parameters were selected based on available tables in the Flo-2d PRO reference manual (Table 3). In particular, with a K_s value of 20 mm h^{-1} the simulated watershed discharge best fits with the precursory shallow-water flow observed in the images, as it will be showed below (Fig. 4). The K_s value of 20 mm h^{-1} is equivalent to the CN value used for the SCS-NC simulations. In fact an empirical relationship between K_s and CN has been proposed by Chong and Teng (1986) as follows:

$$S = 3579 K_s^{1208}, \tag{2}$$

where S is the potential retention related to the CN as follows (Mockus, 1972):

$$CN = \frac{2540}{S + 25.4}. \tag{3}$$

Table 3. Parameters used in the G–A simulations.

Abstraction	6 mm
K_s	20 mm h^{-1}
soil suction	100 mm
initial saturation	0.1
final saturation	0.35

Based on these equations a value of K_s equal to 20 mm h^{-1} corresponds to a CN of 75.5 in the range of values here used for the SCS-NC infiltration model.

The G–A infiltration model was tested in La Lumbre ravine, using the Patricia event and comparing the simulated watershed discharge curve with the available video images. Figure 4 shows the discharge curve that best fits the data gathered from the images, based on which the two methods were qualitatively calibrated. The G–A infiltration method nicely reproduces the initial scouring of muddy water, corresponding with the first increase in the simulated watershed discharge. The SCS-CN infiltration model is not able to reproduce this first water runoff. This can be explained consid-

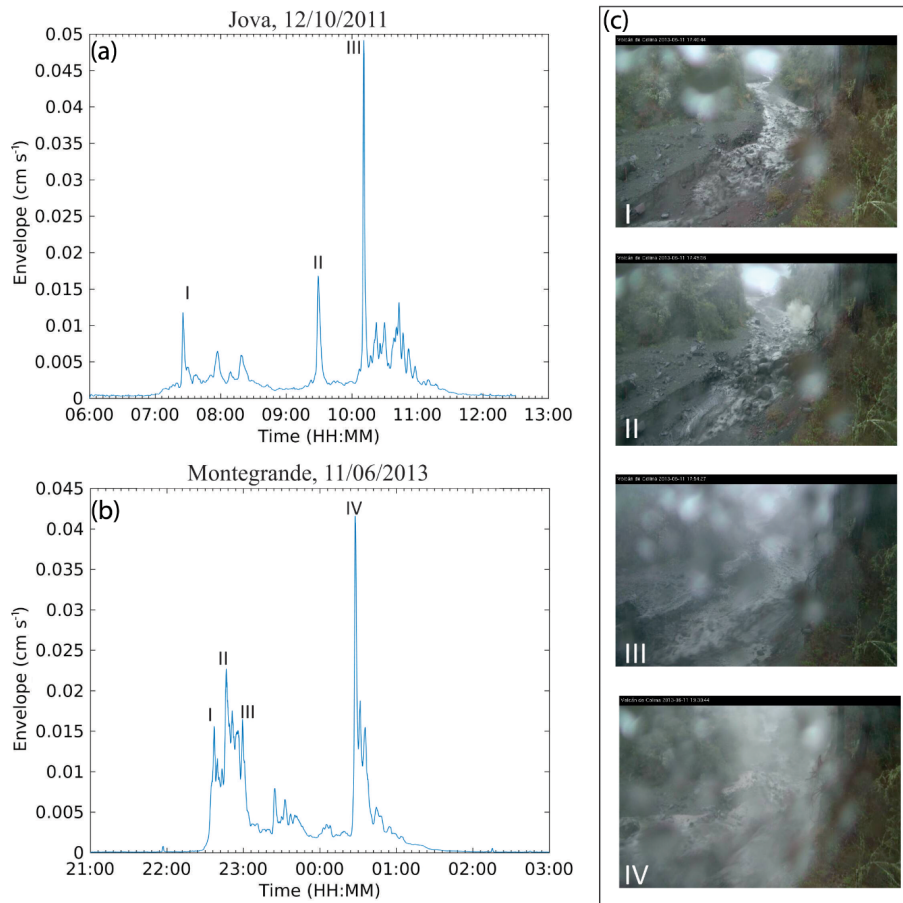


Figure 5. (a) Seismic record of the lahar triggered during the Hurricane Jova, on 12 October 2011. (b) Seismic record of the lahar triggered during the 11 June 2013 event. Main pulses are indicated with roman letters. (c) Images captured by the camera, corresponding to the main lahar pulses as indicated in panel (b).

ering that the initial abstraction due to the interception, infiltration and surface storage, is automatically computed in the SCS-NC method as $0.2S$, probably being too high for the studied area. In contrast, with the G–A method, the initial abstraction can be modified, and best results were obtained with a value of 6 mm corresponding to a surface typical of a vegetated mountain region. However, both infiltration models give similar results for the main peaks of the simulated maximum watershed discharge that correspond to the arrival of the main lahar pulses observed in the images (Fig. 4). These results show that the G–A model is much more reliable to detect precursory slurry flows, while both models are equally able to catch the main surges of a lahar. One important point is that the simulations are here used to set up an EWS to forecast the lag time of the main lahar surges. The first slurry flows were important to calibrate the G–A simulation but they do not represent an essential data for the EWS. In addition, input data for the G–A method often are difficult to set, requiring great care in their measurement. In contrast, the output of the SCS-CN method only depend from

the CN value. The SCS-CN method has been largely used in rainfall-runoff modeling, and we consider that it is a valuable method for the objective of the present work, as we are not seeking a quantitative estimation of the watershed discharge but the arrival times of the main lahar pulses.

A sensitive analysis of the G–A input parameters presented in previous works (i.e., Chen et al., 2015) shows that the saturated hydraulic conductivity K_s is a key factor in the estimation of infiltration rates and exerts a notable influence on runoff calculations (i.e., Chen et al., 2015). With respect to the SCS-CN model, the only input parameter is the CN, thus we present a simple comparison for the Patricia event at La Lumbre ravine. Results obtained with the 80/75 CN values for channel and vegetated area respectively, are compared to two other simulations performed using global values of 75 and 80 (Table 4). This exercise shows that the uncertainty in simulated maximum peak discharge is in the range of 0.1 h, indicating that a global CN value could also be used for the Volcán de Colima.

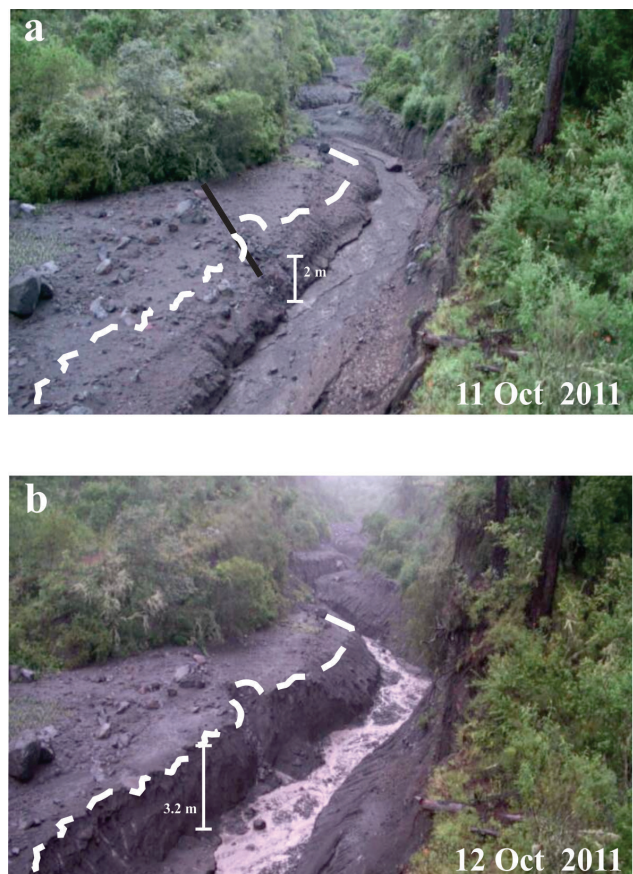


Figure 6. Images showing the morphology of the channel at the monitoring site of the Montegrando ravine (a) the day before and (b) the day after Hurricane Jova.

3 Results

During Hurricane Jova, lahars started at around 07:20 GMT (all times here after reported as GMT) in the Montegrando ravine after ca. 40 % of the total rain (240 mm) had fallen (Fig. 5a). The event lasted more than 4 h, and three main peaks in amplitude can be detected in the seismic signal (Fig. 5a). The first two peaks are similar in amplitude (0.015 cm s^{-1}) and separated by more than 2 h of signal fluctuation. Less than 1 h after from the second peak, a single, discrete pulse can be recognized (0.05 cm s^{-1} in amplitude), followed by a “train” of low-amplitude seismic peaks that lasted for more than an hour.

Along the same ravine, an extreme event was recorded on 11 June 2013 and is introduced here to better discuss the hydrological response of the Montegrando ravine. It represents an unusual event at the beginning of the rainy season, with 120 mm of rain falling in less than 3 h (Table 2), and a maximum peak intensity of 140 mm h^{-1} (Fig. 5b). Based on the seismic record and still images of the event, this lahar was previously characterized as a multi-pulse flow, with three main block-rich fronts (I, II and IV, Fig. 5c), with sim-

Table 4. Arrival times of peak III and IV using different CN values.

Surges observed in the images	Peak III (23.5 h)	Peak IV (24 h)
CN	Arrival times (h) in the simulated watershed discharge curves	
75 global	23.4	24.1
80/75 (channel/vegetated)	23.5	24.1
80 global	23.5	24.2

ilar amplitudes ($0.015\text{--}0.025 \text{ cm s}^{-1}$), followed by a main flow body consisting of a homogenous mixture of water and sediment (with a sediment concentration at the transition between a debris flow and an hyperconcentrated flow) (III, Fig. 5c) (Vázquez et al., 2016a). The last, more energetic pulse (0.042 cm s^{-1}) was accompanied by a water-rich frontal surge that was able to reach the lens of the camera (IV, Fig. 5c). For both Jova and the 11 June 2013 event, the largest pulse corresponds with the final one. Flow discharge was estimated for the 11 June 2013 event, with a maximum value of $120 \text{ m}^3 \text{ s}^{-1}$ for the largest pulse (IV, Fig. 5b) (Vázquez et al., 2016a). For the Jova event, the only visual data available are images of the channel the day before and the day after the event, where deep erosion is visible (Fig. 6). Comparing its seismic signal with the 11 June 2013 lahar, and based on the classification criterion established for lahars at Volcán de Colima (Vázquez et al., 2016a) each main peak is inferred to correspond to the arrival of a flow surge or block-rich front followed by the body of the flow.

The lahar recorded during Hurricane Manuel along the Montegrando ravine shows a similar behavior to that described for the Jova event (Fig. 7). As it occurred during the night no images are available. Based on the seismic record from the BB-RESCO, lahars started at ca. 03:00 and lasted for 7 h. The event was characterized by five main pulses, whose amplitude increases with time ($0.012\text{--}0.025 \text{ cm s}^{-1}$), with the last being the largest in magnitude (0.04 cm s^{-1}). Based on the amplitude values, the first two peaks correspond to precursory dilute flow waves followed by the three main pulses with block-rich fronts (I, II and III, Fig. 7).

In the case of Hurricane Patricia, seismic data (from the geophone) and still images were recorded at the La Lumbre monitoring station. Based on these data, at ca. 16:25 a slurry flow starts on the main channel (Fig. 4). The initial water flow rapidly evolved in a hyperconcentrated flow (Coviello et al., 2018) and several front waves were observed during flooding (I and II, Fig. 8b) for which an average flow discharge of $80\text{--}100 \text{ m}^3 \text{ s}^{-1}$ was estimated, and two main pulses arrived at 23:30 and 00:00 (24 October), with 6 m depth block-rich fronts and maximum flow discharges of $900 \text{ m}^3 \text{ s}^{-1}$ (III, IV, V and VI, Fig. 8b). At around 00:40 the seismic record detected the arrival of a third pulse. Although no images were available, the amplitude of the last pulse (0.07 cm s^{-1}) sug-

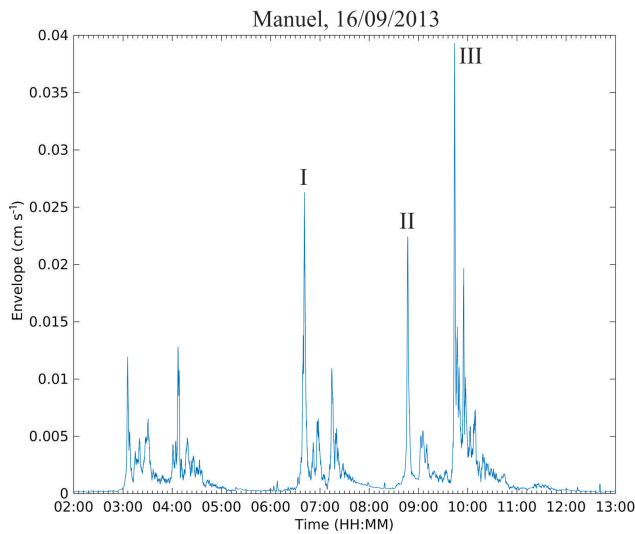


Figure 7. Seismic record of the lahar triggered during Hurricane Manuel, on 15 September 2013, recorded along the Montegrande ravine.

gests it was larger than those previously described. As observed for the three previous events recorded at Montegrande ravine, the largest pulse again corresponded to the last one.

The results of the rainfall-runoff simulation are plotted as a normalized curve of the total runoff hydrograph (watershed discharge), along with the normalized accumulated rainfall and its intensity (calculated over a 10 min interval) (Fig. 9). In the same plot, the arrival time of the main lahar pulses analyzed here is also indicated (red triangles, Fig. 9). By comparing the simulated watershed discharge with rainfall intensity, a general correlation can be observed for the Montegrande basin during hurricane Jova and Manuel (Fig. 9a and b), contrasting with the 11 June 2013 event (Fig. 9c), where the simulation is not able to reproduce watershed discharge during the first minutes of the event when most of rainfall is accumulated and maximum rainfall intensities are detected.

If the arrival times of the main lahar pulses are considered, the events associated with hurricane Jova and Manuel along the Montegrande ravine show a similar behavior. In both cases, early slurry flows are detected after $\sim 40\%$ of the total rain has accumulated. The main flow pulses better correlate with the highest rain intensity values, which also correspond with maximum peaks in simulated watershed discharge; the last, largest pulse corresponds with the maximum simulated peak discharge of the watershed. Finally, analyzing the simulation in the Montegrande ravine for the 11 June 2013 event, it is possible to observe different behavior. The lahar starts as less than the 10% of rain is accumulated, the main lahar pulses perfectly correlate with the peak rainfall intensities, and only the last largest pulse correlates with the watershed peak discharge. For the La Lumbre watershed in 2015, a clear correlation between peak rainfall intensities and simu-

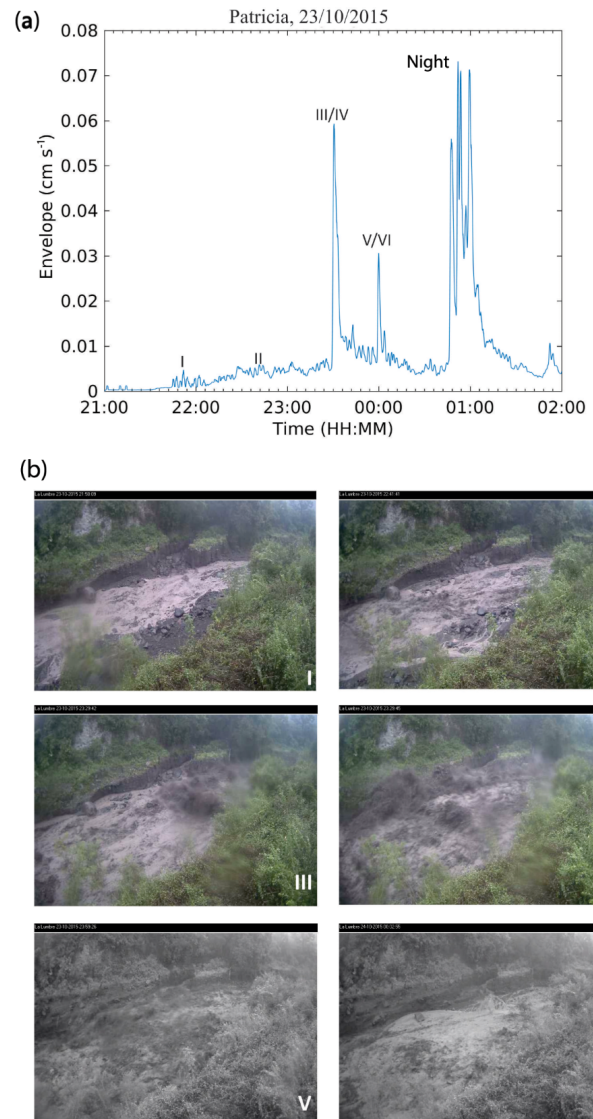


Figure 8. (a) Seismic record of the lahar triggered during Hurricane Patricia, on 26 October 2015, recorded along La Lumbre ravine. The main lahar pulses are indicated with roman numerals. (b) Images captured by the camera, corresponding to the main pulses, as indicated in panel (a).

lated watershed discharge is not clear. For the Patricia event, along the La Lumbre ravine, the first slurry flows (pulse I, Fig. 7b) also start after 40% of total rainfall, but the main lahar pulses fit better with the simulated peaks watershed discharge (Fig. 9d).

4 Discussion

Various attempts have been made to define lahar initiation rainfall thresholds at different volcanoes (i.e., Lavigne et al., 2000; van Westen and Daag, 2005; Barclay et al., 2007; Jones et al., 2015, 2017), including Volcán de Colima (Capra et al.,

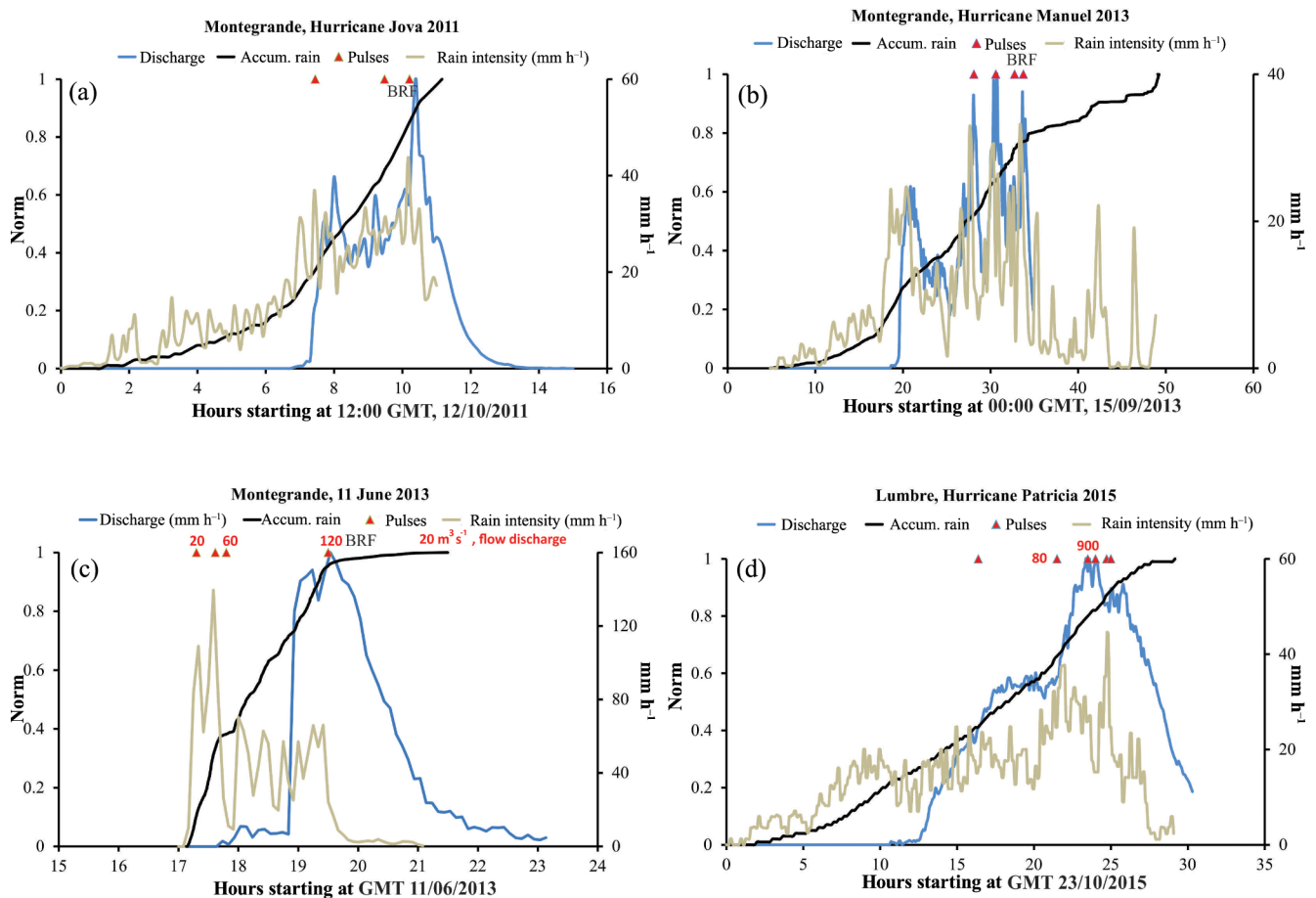


Figure 9. Diagrams showing the main lahar pulses (red triangles) as detected from the seismic signal of the analyzed events in relation with the accumulated rainfall (dark line), rainfall intensity (10 m h^{-1}) (gray line) and simulated watershed discharge (blue line) for the following hydro-meteorological events (a) Jova; (b) Manuel; (c) 11 June 2013; and (d) Patricia.

2010). This study focused on better prediction of lahar evolution during extraordinary hydro-meteorological events such as hurricanes, a common long-duration and large-scale rainfall phenomenon in tropical latitudes. In particular, we are interested in predicting the arrival of block-rich flow fronts that have caused severe damage during past events. Based on the seismic and visual data gathered from the events analyzed here, it is possible to identify the key factors in controlling the arrival timing of main lahar fronts. For the Jova, Manuel and Patricia events, lahars started after the 40% of total rain had accumulated (corresponding to ca. 100, 120 and 160 mm of rain respectively), and the timing for the main pulses correlates well with the peaks of the rainfall intensity for the Montegrando ravine, while for La Lumbre ravine they better match with the peaks of the simulated watershed discharge. The observed differences between Montegrando and La Lumbre ravines can be correlated with the different areas and shapes of the two catchments. In fact, due to its elongated shape ($K_G = 1.7$ and small area (2 km^2), the Montegrando watershed shows a quicker response between rain-

fall and discharge, with rapid water concentration at different points along the main channel (Fig. 1b). This behavior is much clearer for the 11 June 2013 event, which occurred at the beginning of the rain season when soils on the lateral terraces of the ravines show hydrophobic behavior (Capra et al., 2010). The simulation was not able to reproduce any watershed discharge at the beginning of the event, because the hydrophobic behavior of the soils inhibits the infiltration and the water runoff quickly promotes lahar initiation. During this event, the first lahar pulses perfectly match with the rainfall peak intensities (except for the last major pulse), starting from the very beginning of the rainfall event. In contrast, La Lumbre ravine has a wider, rounded upper watershed ($K_G = 1.1$; $A = 14 \text{ km}^2$) that is able to concentrate a larger volume of water entering the main channel where lateral contributions still increase water discharge further. Even if rain during hurricanes Manuel and Patricia showed similar behavior (Fig. 3), the catchment response of La Lumbre is clearly different with a pulsating behavior of lahars mainly controlled by the watershed discharge. Nevertheless, for all

the events analyzed here, the largest pulse corresponds with the last one recorded and it correlates with the maximum simulated watershed discharge, pointing to strong control of catchment recharge, in generating the largest and most destructive pulses. Previous works correlated the occurrence of surges within a lahar to multiple sources, such as lateral tributaries along the main channel (i.e., Doyle et al., 2010) or due to the failure of temporary dams of large clasts triggered by an increase in rainfall intensity (Kean et al., 2013). Lateral tributaries are absent in both the Montegrando and La Lumbre channels, and even if an accumulation of clasts were possible, no significant discontinuities of the channel bed can be observed upstream of the monitoring sites. Based on data presented here, formation of pulses within a lahar is mostly controlled by the watershed shape that regulates the timing of the arrival of main pulses, depending on the rainfall behavior. Nevertheless, the last pulse is always the largest in volume.

This model is strictly related to long-duration and large-scale rainfall events hitting tropical volcanoes, such as the Volcán de Colima. In contrast, during mesoscale non-stationary rainfall typical at the beginning of the rainy season, lahars are usually triggered at low accumulated rainfall values and controlled by rainfall intensity due to the hydrophobic behavior of soils, and they usually consist of single-pulse events with one block-rich front that lasts less than 1 h (i.e., Vázquez et al., 2016b). In perspective, the results presented here can be used to design an EWS for hurricane-induced lahars, i.e., events triggered by long-duration and large-scale rainfalls. The most common pre-event or advanced EWSs for debris flows are based on empirical correlations between rainfall and debris flow occurrence (e.g., Keefer et al., 1987; Aleotti, 2004; Baum and Godt, 2009; Jones et al., 2017; Wei et al., 2017; Greco and Pagano, 2017). The instruments adopted for debris-flow advance warning are those normally used for hydro-meteorological monitoring and consist of telemetry networks of rain gauges and/or weather radar. The typical way to represent these relations is identifying critical rainfall thresholds for debris flow occurrence. The availability of both a large catalogue of events and a reliable precipitation forecast, that could give the predicted amount of rainfall some hours in advance, would allow the issue of an effective warning, at least in predicting the likely arrival time of the main lahar pulses. In addition, instrumental monitoring of in-channel processes can be used to validate a preliminary warning-condition triggered by weather forecast and/or rainfall measurements.

5 Conclusions

Monitoring data from long-lasting lahars triggered by Hurricane Jova, Manuel and Patricia at Volcán de Colima demonstrated that watershed discharge is the key factor in controlling the arrival time of main block-rich fronts, and that the largest destructive pulses will arrive after the initial surges. In

particular, for the 2015 Hurricane Patricia the weather forecast predicted a value of total rainfall, and also the approximate time of its landfall the day before the event. Based on the theoretical rainfall distribution designed with the hydro-meteorological events analyzed here, it would obtain the rainfall and time distribution of the event analyzed here, and it would have been possible to anticipate when lahars started along the La Lumbre ravine and the arrival time of main pulses. This first rough prediction of the arrival times of main lahar pulses could have been validated and updated based on real time data acquisition and rainfall-runoff simulations that do not take more than 30 min to provide results. This information coupled with the real-time monitoring can be a valuable tool to employ for hazard assessment and risk mitigation. These findings can be used to implement an advanced EWS based on the monitoring of a hydro-meteorological process to issue a warning before a possible lahar is triggered.

Data availability. Rain gauge data, images and seismic records are available under a collaborative framework between Centro de Geociencias, UNAM (Lucia Capra) and related universities. Please contact Lucia Capra for any further information. Data is available upon request, based on a collaborative agreement.

Competing interests. The authors declare that they have no conflict of interest.

Special issue statement. This article is part of the special issue “Landslide early warning systems: monitoring systems, rainfall thresholds, warning models, performance evaluation and risk perception”. It does not belong to a conference.

Acknowledgements. This work was supported by CONACyT projects 360 and 220786 granted to Lucia Capra and by the post-doctoral fellowship of DGAPA (Programa de Becas Posdoctorales de la UNAM) granted to Velio Coviello. Thanks to José Luis Ortiz and Sergio Rodríguez, from the Centro de Prevención de Desastres (CENAPRED), who set up the instrumentation on the Montegrando monitoring site.

Edited by: Samuele Segoni

Reviewed by: two anonymous referees

References

- Aleotti, P.: A warning system for rainfall-induced shallow failures, *Eng. Geol.*, 73, 247–265, 2004.
- Barclay, J., Alexander, J., and Susnik, L.: Rainfall-induced lahars in the Belham valley, Monserrat, West Indies, *Journal of the Geological Society of London*, 164, 815–827, 2007.
- Bartolini, D. and Borselli, L.: Evaluation of the HydrologicSoil Group (HSG) with the Procedure SCS Curve Number, in: Man-

- ual of Methods for Soil and Land Evaluation, edited by: Edoardo, A. and Costantini, C., Science Publisher Inc., Enfield, USA, 600 pp., 2009.
- Baum, R. L. and Godt, J. W.: Early warning of rainfall-induced shallow landslides and debris flows in the USA, *Landslides*, 3, 259–272, 2009.
- Bendjoudi, H. and Hubert, P.: Le coefficient de Gravelius: analyse critique d'un indice de forme des bassins versants, *J. Sci. Hydrol.*, 47, 921–930, 2002.
- Capra, L., Borselli, L., Varley, N., Norini, G., Gavilanes-Ruiz, J. C., Sarocchi, D., and Caballero, L.: Rainfall-triggered lahars at Volcán de Colima, Mexico: surface hydro-repellency as initiation process, *J. Volcanol. Geoth. Res.*, 189, 105–117, 2010.
- Capra, L., Macias, J. L., Cortes, A., Saucedo, S., Osorio-Ocampo, S., Davila, N., Arce, J. L., Gavilanes-Ruiz, J. C., Corona-Chávez, P., García-Sánchez, L., Sosa-Ceballos, G., and Vázquez, R.: Preliminary report on the 10–11 July 2015 eruption at Volcán de Colima: Pyroclastic density currents with exceptional runouts and volumes, *J. Volcanol. Geoth. Res.*, 310, 39–49, 2016.
- Chen, L., Xiang, L., Young, M. H., Yin, J., Yu, Z., and van Genuchten, M. T.: Optimal parameters for the Green-Ampt infiltration model under rainfall conditions, *J. Hydrol. Hydromech.*, 63, 93–101, 2015.
- Chong, S. K. and Teng, T. M.: Relationship between the runoff curve number and hydrologic soil properties, *J. Hydrol.*, 84, 1–7, 1986.
- Cortes, A., Macias, J. L., Capra, L., and Garduño-Monroy, V. H.: Sector collapse of the SW flank of Volcán de Colima, México. The 3600 yr BP La Lumbre-Los Ganchos debris avalanche and associated debris flows, *J. Volcanol. Geoth. Res.*, 197, 52–66, 2010.
- Coviello, V., Capra, L., Vaizquez, R., and Marquez-Ramirez, V.: Seismic characterization of hyperconcentrated flows in volcanic environment, *Earth Surf. Proc. Land*, accepted, 2018.
- Davila, N., Capra, L., Gavilanes, J. C., Varley, N., and Norini, G.: Recent lahars at Volcán de Colima (Mexico): drainage variation and spectral classification, *J. Volcanol. Geoth. Res.*, 165, 127–141, 2007.
- de Bélizal, E., Lavigne, F., Hadmoko, D. S., Degai, J. P., Dipayana, G. A., Mutagin, B. W., Marfai, M. A., Coquet, M., Le Mauff, B., Robin, A. K., Vidal, C., Cholik, N., and Aisyah, N.: Rain-triggered lahars following the 2010 eruption of Merapi volcano, Indonesia: A major risk, *J. Volcanol. Geoth. Res.*, 261, 330–347, 2013.
- Doyle, E. E., Cronin, S. J., Cole, S. E., and Thouret, J. C.: The coalescence and organization of lahars at Semeru volcano, Indonesia, *B. Volcanol.*, 72, 961–970, 2010.
- Dumaisnil, C., Thouret, J. C., Chambon, G., Doyle, E. E., and Cronin, S. J.: Hydraulic, physical and rheological characteristics of rain-triggered lahars at Semeru volcano, Indonesia, *Earth Surf. Proc. Land.*, 35, 1573–1590, 2010.
- Ferrer-Julia, M., Estrela, T., Sanchez del Corral Jimenez, A., and Garcia-Melendez, E.: Generation of a curve number map with continuous values based on saturated hydraulic conductivity, XI World Water Congress, 5–9 October 2003, Madrid, Spain, 1–10, available at: <https://www.iwra.org/member/index.php?mainpage=&page=286&congressyear=2003> (last access: 5 March 2018), 2003.
- Gentile, F., Bisantino, T., Puglisi, S., and Trisorio Liuzzi, G.: Analysis and modeling of debris flows in Gargano watersheds (Puglia region, Southern Italy), *Wit. Trans. Ecol. Envir.*, 90, 181–191, 2006.
- Gravelius, H.: Grundrifi der gesamten Gewässerkunde, Band I: Flufkunde (Compendium of Hydrology, Vol. I. Rivers, in German), Goschen, Berlin, Germany, 1914.
- Greco, R. and Pagano, L.: Basic features of the predictive tools of early warning systems for water-related natural hazards: examples for shallow landslides, *Nat. Hazards Earth Syst. Sci.*, 17, 2213–2227, <https://doi.org/10.5194/nhess-17-2213-2017>, 2017.
- Green, W. H. and Ampt, G.: Studies of soil physics, part I – the flow of air and water through soils, *J. Agr. Sci.*, 4, 1–24, 1911.
- Grimaldi, S., Petroselli, A., and Romano, N.: Green-Ampt Curve-Number mixed procedure as an empirical tool for rainfall-runoff modelling in small and ungauged basins, *Hydrol. Process.*, 27, 1253–1264, 2013.
- Hawkins, R. H., Hjelmfelt, A. T., and Zevenbergen, A. W.: Runoff probability storm depth and curve numbers, *J. Irr. Drain. Div.-ASCE*, 111, 330–340, 1985.
- Iverson, R. M.: The physics of debris flows, *Rev. Geophys.*, 35, 245–296, 1997.
- Jones, R., Manville, V., and Andrade, D.: Probabilistic analysis of rain-triggered lahar initiation at Tungurahua volcano, *B. Volcanol.*, 77, 68, 2015.
- Jones, R., Manville, V., Peakall, J., Froude, M. J., and Odbert, H. M.: Real-time prediction of rain-triggered lahars: incorporating seasonality and catchment recovery, *Nat. Hazards Earth Syst. Sci.*, 17, 2301–2312, <https://doi.org/10.5194/nhess-17-2301-2017>, 2017.
- Kean, W., McCoy, S., Tucker, G., Staley, D., and Coe, J.: Runoff-generated debris flows: Observations and modeling of surge initiation, magnitude, and frequency, *J. Geophys. Res.-Earth*, 118, 1–18, 2013.
- Keefer, D. K., Wilson, R. C., Mark, R. K., Brabb, E. E., Brown, W. M., Ellen, S. D., Harp, E. L., Wiczorek, G. F., Alger, C. S., and Zarkin, R. S.: Real-time landslide warning during heavy rainfall, *Science*, 238, 921–925, 1987.
- Lavigne, F. and Thouret, J. C.: Sediment transport and deposition by rain-triggered lahars at Merapi Volcano, Central Java, Indonesia, *Geomorphology*, 49, 45–69, 2002.
- Lavigne, F., Thouret, J. C., Voight, B., Suwa, H., and Sumaryono, A.: Lahars at Merapi volcano, Central Java: an overview, *J. Volcanol. Geoth. Res.*, 100, 423–456, 2000.
- Llanes, F., Ferrer, P. K., Gacusan, R., Realino, V., Obrique, J., Eco, R. N., and Lagmay, A. M. F.: Scenario-based maps using flood2d and IFSAR-derived digital elevation models on the November 2006 rainfall-induced lahars, Mayon Volcano, Philippines, ACRS 2015 Proceedings, Asian Association on Remote Sensing, 2015.
- Marchi, L., Arattano, M., and Deganutti, A.: Ten years of debris-flow monitoring in the Moscardaro Torrent (Italian Alps), *Geomorphology*, 46, 1–17, [https://doi.org/10.1016/S0169-555X\(01\)00162-3](https://doi.org/10.1016/S0169-555X(01)00162-3), 2002.
- Mishra, S. K. and Singh, V. P.: Soil conservation service curve number (SCS-CN) methodology, Kluwer Academic Publishers, Dordrecht, the Netherlands, 2003.

- Mockus, V.: Estimation of direct runoff from storm rainfall national engineering handbook, Soil Conservation Service, Washington, DC, 1972.
- NRCS-Natural Resource Conservation Services: Rainfall-Frequency and Design Rainfall Distribution for Selected Pacific Islands, Engineering Technical Note No. 3, United States Department of Agriculture, 115 pp., 2008.
- O'Brien, J., Julien, P., and Fullerton, W.: Two-dimensional water flood and mudflow simulation, *J. Hydraul. Eng.-ASCE*, 119, 244–261, 1993.
- Ortiz-Rodríguez, A. J., Borselli, L., and Sarocchi, D.: Flow connectivity in active volcanic areas: use of index of connectivity in the assessment of lateral flow contribution to main streams, *Catena*, 157, 90–111, 2017.
- Ponce, V. and Hawkins, R.: Runoff curve number: Has it reached maturity?, *J. Hydrol. Eng.*, 1, 11–19, 1996.
- Rallison, R. E.: Origin and evolution of the SCS runoff equation, in: *Proc. ASCE Irrigation and Drainage Div., Symp. on Watershed Management, Vol. II*, ASCE, New York, NY, 912–924, 1980.
- Roverato, M., Capra, L., Sulpizio, R., and Norini, G.: Stratigraphic reconstruction of two debris avalanche deposits at Colima Volcano (Mexico): Insights into pre-failure conditions and climate influence, *J. Volcanol. Geoth. Res.*, 207, 33–46, 2011.
- Scott, K. M., Vallance, J. V., Kerle, N., Macias, J. L., Strauch, W., and Devoli, G.: Catastrophic precipitation-triggered lahars at Casita Volcano, Nicaragua: occurrence, bulking and transformation, *Earth Surf. Proc. Land.*, 30, 59–79, 2005.
- Sheridan, M. F., Connor, C. B., Connor, L., Stinton, A. J., Galacia, O., and Barrios, G.: October 2005 Debris Flows at Panabaj, Guatemala: Hazard Assessment, American Geophysical Union, Spring Meeting 2007, abstract #V33A-07, 2007.
- Takahashi, T.: Debris Flow: Mechanics Prediction, and Countermeasures, Taylor and Francis/Balkema, Leiden, 572 pp., 2007.
- Umbal, J. V. and Rodolfo, K. S.: The 1991 lahars of southwestern Mount Pinatubo and evolution of the lahar-dammed Mapanuepe lake, in: *Fire and mud, eruptions and lahars of Mount Pinatubo, Philippines*, Philippine Institute of Volcanology and Seismology, Quezon, Philippines, 951–970, 1996.
- USDA-NRCS (U.S. Department of Agriculture-Natural Resources Conservation Service), Hydrologic soil groups, National engineering handbook, Part 630, Hydrology, Washington, DC, 2007.
- van Westen, C. J. and Daag, A. S.: Analysing the relation between rainfall characteristics and lahar activity at Mount Pinatubo, Philippines, *Earth Surf. Proc. Land.*, 30, 1663–1674, 2005.
- Van Wyk Vries, B., Kerle, N., and Petley, D.: Sector collapse forming at Casita volcano, Nicaragua, *Geology*, 28, 167–170, 2000.
- Vázquez, R., Suriñach, E., Capra, L., Arámbula-Mendoza, R., and Reyes-Dávila, G.: Seismic characterisation of lahars at Volcán de Colima, Mexico, *B. Volcanol.*, 78, 8, 2016a.
- Vázquez, R., Capra, L., and Coviello, V.: Factors controlling erosion/deposition phenomena related to lahars at Volcán de Colima, Mexico, *Nat. Hazards Earth Syst. Sci.*, 16, 1881–1895, <https://doi.org/10.5194/nhess-16-1881-2016>, 2016b.
- Wei, L.-W., Huang, C.-M., Lee, C.-T., Chi, C.-C., and Chiu, C.-L.: Adopting I_3-R_{24} rainfall index and landslide susceptibility on the establishment of early warning model for rainfall-induced shallow landslides, *Nat. Hazards Earth Syst. Sci. Discuss.*, <https://doi.org/10.5194/nhess-2017-428>, in review, 2017.
- Zanuttigh, B. and Lamberti, A.: Instability and surge development in debris flows, *Rev. Geophys.*, 45, RG3006, <https://doi.org/10.1029/2005RG000175>, 2007.
- Zobin, V. M., Placencia, I., Reyes, G., and Navarro, C.: The characteristics of seismic signal produced by lahars and pyroclastic flows: Volcán de Colima, Mexico, *J. Volcanol. Geoth. Res.*, 179, 157–167, 2009.